Al-Mukhtar Journal of Basic Sciences 24 (2): 173-184, 2026
Doi: https://doi.org/10.54172/k56j7q87

Research Article **Open Access**

Adsorption Isotherm and Kinetic Studies of Copper(II) Removal from Aqueous Solutions Using Graphene Oxide

Raja Izriq[1]*, Rokaya Azaga[2], Mohammed S. Ibrahim[3] and Hamd Moamen[4]

***Corresponding author:** raja.krifiet@sebhau.edu.ly , Department of Chemistry, Faculty of Science, Sebha University, Libya.

[2, 3, 4] Department of Chemistry, Faculty of Science, Sebha University, Libya.

Received:
21 June 2026

Accepted:
28 August 2026

Publish online:
31 August 2026

Abstract
Graphene oxide (GO) exhibits good chemical stability for water purification applications. GO contains abundant oxygen-containing functional groups, such as hydroxyl, epoxy, and carboxyl moieties, which provide active adsorption sites. These features enable the effective capture of pollutants. In this study, GO was used as an adsorbent to remove Cu(II) ions from aqueous solutions. GO was prepared from graphite using a modified Hummers method and characterized using FT-IR and XRD techniques. Cu(II) adsorption onto GO was evaluated using an atomic absorption spectrophotometer (AAS). The kinetic parameters were determined using pseudo-first-order and pseudo-second-order kinetic models; the results showed that the adsorption process followed the pseudo-second-order kinetic model. The Langmuir, Freundlich, and Temkin isotherm models were applied, with a maximum adsorption capacity of 324 $mg.g^{-1}$. Thermodynamic parameters, including ΔG◦, ΔH◦, and ΔS◦, were calculated, indicating that the adsorption process was spontaneous and endothermic.

Keywords: Graphene Oxide; Heavy Metals; Adsorption; Adsorption Capacity; Kinetics; Thermodynamic Parameters

INTRODUCTION

In recent years, contamination by heavy metals has emerged as a significant concern for both environmental integrity and global public health. Human exposure to these metals has increased markedly due to their widespread and rapidly expanding use in industrial, agricultural, domestic, and technological applications (Elewa et al., 2023). Contamination of water by heavy metal ions is a major environmental concern because it directly affects human health and other living organisms. Heavy metal ions such as mercury, copper, iron, nickel, and lead are not biodegradable; therefore, they can persist in the environment for long periods, bioaccumulate, and cause various diseases and health problems (Ahmed, Choudhury, Alam, & Nurnabi, 2023; Imamoglu & Tekir, 2008). The harmful effects of heavy metals stem from their ability to interfere with the body's biochemical processes, leading to health problems such as diarrhea, liver and kidney damage, Alzheimer's disease, hypertension, and cancer (Ali et al., 2023; Nassef, Al-Hazmi, Alayyafi, El-Desouky, & El-Bindary, 2024).

Copper is an essential trace element in living organisms. At low concentrations, it participates in several biological processes, including erythropoiesis and the functioning of the nervous and immune systems. Furthermore, Cu(II) is important for healthy brain development. Nevertheless, excessive accumulation of copper may lead to severe toxic effects because of its persistent and non-degradable nature, causing liver damage and neurological disorders (Katiyar et al., 2021). Accordingly, copper is considered a toxic heavy metal that does not degrade in the environment, poses risks to human health, and is not easily metabolized by the human body. Major sources of copper-containing waste include effluents from electroplating and textile industries, as well as wastewater generated during the remediation of copper-contaminated soils, therefore, these waste streams must be treated and controlled to acceptable levels before being discharged into the environment (White, White, Turgut, Massoud, & Tian, 2018). To date, many techniques have been used for water treatment and heavy metal removal. These methods are designed to remove harmful metal ions from contaminated water, thereby improving water quality and protecting public health. Conventional methods include chemical precipitation (Benalia, Youcef, Bouaziz, Achour, & Menasra, 2022), membrane filtration (Dawam, Gobara, Oraby, Y. Zorainy, & Nabil, 2025), electrochemical treatment (Deng et al., 2022), ion exchange (Shek, Ma, Lee, & McKay, 2009), and adsorption (Türkmen, Bakhshpour, Akgönüllü, Aşır, & Denizli, 2022). However, some of these treatment methods have notable limitations, including high chemical and energy consumption, elevated costs at large-scale operations, and reduced efficiency when metal concentrations fall below 100 $mg.L^{-1}$ (Ayach et al., 2024; Türkmen et al., 2022).

Among various treatment methods, adsorption is a simple and effective method widely used in wastewater treatment, where different types of adsorbent materials are applied to remove contaminants (Khan, Muhammad, AlOthman, Cheong, & Ali, 2022). Adsorption is often preferred because of its simple design, process efficiency, and low overall cost (Raji, Karim, Karam, & Khalloufi, 2023). A range of adsorbents, including alumina and bauxite, silica gel, zeolites, ion-exchange resins, activated carbon, and nano-adsorbents, have been employed in water treatment and remediation (Dutta, Gupta, Srivastava, & Gupta, 2021; Gupta, Carrott, Ribeiro Carrott, & Suhas, 2009). Nanomaterials have attracted widespread interest because their properties differ from those of conventional materials. These materials possess unique optical and catalytic properties that are highly dependent on nanoparticle size and shape (Abu-Dief, Abdel-Rahman, Abd–ElSayed, & Zikry, 2021). Graphene oxide (GO) has been extensively utilized as a high-performance adsorbent for removing contaminants and heavy metal ions from water (Abu-Dief et al., 2021). GO is a highly oxidized, two-dimensional derivative of graphene, often described as oxidized graphite sheets, and is produced through the chemical oxidation of natural graphite (Hu et al., 2013). GO is characterized by the coexistence of sp^2 (aromatic) and sp^3 (aliphatic) carbon domains. This structural heterogeneity enhances its surface chemistry and significantly expands the range of possible interactions with surrounding species (Deshwal et al., 2023). Unlike pristine graphite, GO sheets contain a high concentration of oxygen-containing functional groups. These include hydroxyl and epoxide groups distributed across the basal planes, as well as carbonyl and carboxyl groups located at the sheet edges. The presence of these functional groups, along with the large surface area of GO, makes it highly promising for the removal and recovery of metal ions from aqueous solutions (Deshwal et al., 2023). Researchers have increasingly directed their attention toward the use of GO and its functionalized derivatives as effective adsorbent materials for the removal of toxic metal ions from aqueous environments. In this context, several studies have demonstrated the high adsorption capacity and efficiency of these materials for removing hazardous heavy metals from water systems (Gomes et al., 2022; Kumar & Jiang, 2016; Rathore & Biswas, 2018). Several studies have investigated GO for the removal of Cu(II) from aqueous solutions and have identified two main approaches to its use in adsorption processes. The first involves the application of pure GO, while the second focuses on GO modified with various materials to enhance its adsorption capacity and selectivity (Yi et al., 2017). For example, Wu et al. prepared GO using a modified Hummers method and used it as an adsorbent for Cu(II) removal from aqueous solution. The results showed that the maximum adsorption capacity was 117.5 mg.g−1 (W. Wu et al., 2013). In another study, GO was synthesized from graphite powder using a modified Hummers method, followed by carboxylation to obtain GO–COOH. The carboxylation process was carried out in a strongly basic medium by reacting chloroacetic acid with sodium hydroxide (NaOH). Subsequently, both GO and GO–COOH were systematically characterized and used to remove Cu(II) from aqueous solution; their maximum adsorption capacities were 277.77 and 357.14 mg.g-1, respectively (White et al., 2018). In the present study, GO powder was prepared using the Hummers method and evaluated for its efficiency in removing Cu(II) from aqueous media. GO was characterized by Fourier-transform infrared spectroscopy (FT-IR) and X-ray diffraction (XRD), and Cu(II) adsorption onto GO was evaluated using an atomic absorption spectrophotometer (AAS). The adsorption behavior of Cu(II) was evaluated using different kinetic and isotherm models.

MATERIALS AND METHODS

Materials

Graphite powder was obtained from Philip Harris (UK); sulfuric acid (H2SO4, 98%), hydrochloric acid (HCl, 37%), potassium permanganate (KMnO4), and hydrogen peroxide (H2O2, 30%) were obtained from Carlo Erba (France); and copper sulfate (CuSO4) was obtained from Alfa Aesar (Germany).

Synthesis of Graphene Oxide

The modified Hummers method was used to synthesize GO (Chen, Li, Huang, Li, & Shi, 2015). In a 500 mL beaker, 2 g of powdered graphite was mixed with 46 mL of concentrated sulfuric acid. The mixture was mechanically stirred continuously while maintained in an ice bath. Potassium permanganate (6 g) was added slowly to the mixture while the temperature was maintained below 15 °C. The ice bath was removed, and the mixture was stirred at 40 °C for half an hour. Subsequently, 100 mL of distilled water was added very slowly (the reaction is exothermic, so caution is required at this step), and the mixture was stirred for 15 minutes at 98 °C. A further 300 mL of distilled water was added to the mixture, followed by the dropwise addition of 10 mL of hydrogen peroxide (30%) to terminate the reaction; the colour changed from dark brown to yellow. The mixture was washed several times with 0.1 M HCl solution and water using centrifugation to remove ions. Afterward, 600 mL of water was added, and the mixture was stirred for 12 hours and then placed in an ultrasound machine for 1 hour to facilitate exfoliation. The exfoliated portion was separated and dried at 45 °C to obtain GO.

Characterization

Fourier-transform infrared (FT-IR) spectra of GO were recorded using a Bruker Tensor 27 FT-IR spectrometer over a wavenumber range of 400–4000 cm-1. X-ray diffraction (XRD) analysis was carried out using an Empyrean Malvern Panalytical diffractometer with Cu Kα radiation (= 0.154059 nm).

Adsorption Experiments

Copper sulfate was dissolved in distilled water to prepare a stock solution of Cu(II) ions at a concentration of 500 mg.L^{-1}. The pH of the prepared solution was measured and found to be 5. To investigate Cu(II) adsorption onto GO, 1 mg of GO was added to 100 mL of Cu(II) solutions at different initial concentrations (1 to 10 mg.L^{-1}) for isotherm studies, and the suspensions were shaken for different contact times (1 to 240 min) for kinetic studies. All experiments were conducted at 25 °C, except those performed at 35, 45, and 55 °C to determine the thermodynamic parameters. Following filtration, the residual concentration of Cu(II) ions was determined using an atomic absorption spectrophotometer (AAS) (NovAA 400, Analytik Jena, Germany).

The adsorption capacity q_e ($mg.g^{-1}$) was calculated from the following equation:

$$q_e = \frac{(C_0 - C_e)\,V}{m} \qquad (1)$$

where C_0 is the initial concentration ($mg.L^{-1}$) of Cu(II), Ce is the equilibrium concentration of unadsorbed Cu(II) ($mg.L^{-1}$), V is the solution volume (L), and m is the mass of graphene oxide (g).

RESULTS AND DISCUSSION

Characterization

The XRD pattern of GO is shown in Figure 1. A peak at 2θ = 12.38° is a distinctive feature of GO. The high peak intensity indicates a high proportion of GO in the sample. The interlayer distance (d-spacing) was calculated using Bragg's equation and was 0.71 nm, consistent with values reported in the literature (Liu, Zhong, & Zhang, 2015; Shalaby et al., 2015; Xue, Zhu, Liu, & Li, 2015). In Figure 1, the absence of the characteristic peak of pure graphite, which appears at approximately 2θ = 26°, was observed, indicating complete oxidation of the graphite (Guerrero-Contreras & Caballero-Briones, 2015; Kaushal, Dhawan, & Singh, 2019). The figure also shows a relatively broad, weak feature or small peaks around 42–44°, indicating turbostratic disorder (Emiru & Ayele, 2017; Vieira et al., 2016; Viprya, Kumar, & Kowshik, 2023). The FT-IR spectrum of GO is shown in Figure 2 and was recorded over the range of 4000–400 cm-1. The characteristic GO peaks at 3409, 1704, 1612, 1388, and 1126 cm-1 are attributed to O–H stretching, C=O stretching, C=C stretching, O–H bending, and C–O stretching of the epoxy group, respectively (Marcano et al., 2010).

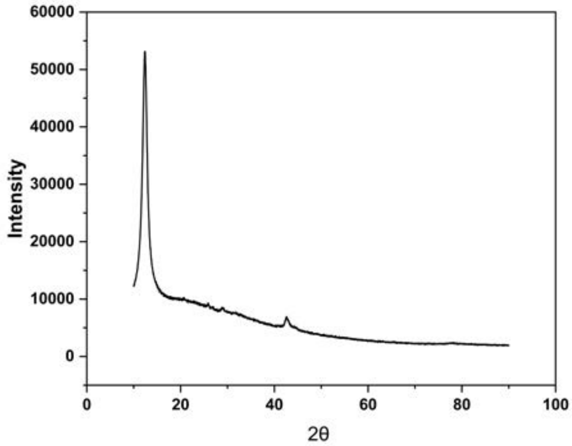

Figure (1). XRD pattern of GO.

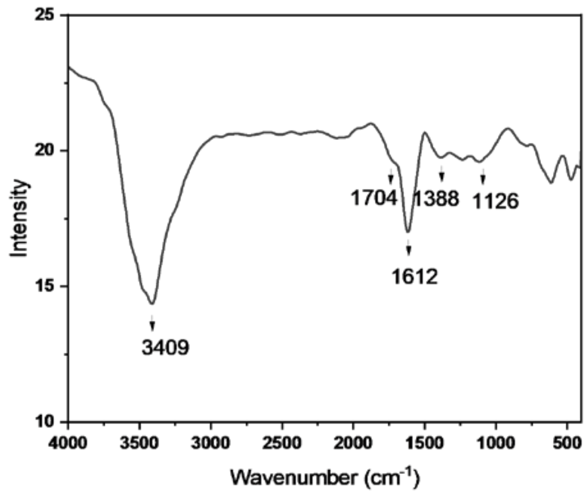

Figure (2). FT-IR spectrum of GO.

Adsorption Kinetics

To investigate the adsorption kinetics of Cu(II) (5 mg.L^{-1}) onto GO (1 mg), the pseudo-first-order and pseudo-second-order models were applied using the following equations.

The pseudo-first-order model:

$$ln(q_e - q_t) = lnq_e - k_1 t \qquad (2)$$

The pseudo-second-order model:

$$\frac{t}{q_t} = \frac{1}{k_2 q_e^2} + \frac{t}{q_e} \qquad (3)$$

where q_e is the adsorption capacity at equilibrium, q_t is the amount adsorbed at time t (min), and k1 (min^{-1}) and k_2 (g mg^{-1} min^{-1}) are the rate constants of the pseudo-first-order and pseudo-second-order kinetic equations, respectively. Figure 3 shows the corresponding linear plots for the pseudo-first-order model (Figure 3a) and the pseudo-second-order model (Figure 3b), respectively. The rate constants $ln(q_e - q_t)\frac{t}{q_t}k_1$ and k_2 obtained from the plots were 0.0499 min^{-1} and 0.005 g mg^{-1} min^{-1}, respectively. The correlation coefficient (R^2) of the pseudo-first-order model was 0.989, whereas that of the pseudo-second-order model was 0.997. The calculated q_e value for the pseudo-first-order model was 46.13 mg.g^{-1}, whereas the value for the pseudo-second-order model was 115.47 mg.g^{-1}, which is close to the experimental value of 116 mg.g^{-1}. The kinetic constants and the q_e and R^2 values are presented in Table 1. As shown in Table 1, the correlation coefficient (R^2) of the pseudo-second-order model was higher than that of the pseudo-first-order model, confirming the applicability of the pseudo-second-order equation.

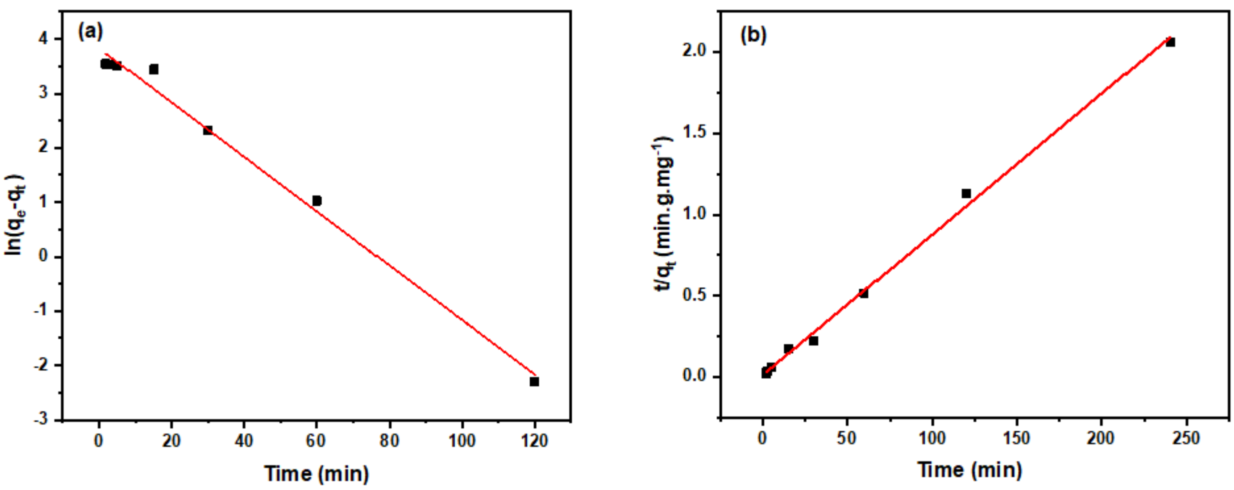

Figure (3). (a) Pseudo-first-order model and (b) pseudo-second-order model for adsorption of Cu(II) onto GO.

Table (1). Parameters for the kinetic models

Parameter	pseudo-first-order model	pseudo-second-order model
k	0.0499 min^{-1}	0.005 g mg^{-1} min^{-1}
q_e	46.13 (mg.g^{-1})	115.47 mg g^{-1}
R^2	0.989	0.997

Adsorption Isotherms

Cu(II) adsorption experiments using 1 mg of GO were conducted at 25 °C. The Langmuir, Freundlich, and Temkin isotherm models were used to analyze the experimental data.

The Langmuir isotherm model assumes that adsorption occurs at specific homogeneous sites within an adsorbent and, once an adsorbate occupies a site, no further adsorption can occur on that site. The Langmuir isotherm is expressed mathematically as follows (Musah et al., 2022):

$$\frac{c_e}{q_e} = \frac{1}{q_m K_L} + \frac{c_e}{q_m} \qquad (4)$$

where qe is the adsorption capacity (mg.g-1), q_m is the maximum monolayer adsorption capacity, C_e is the equilibrium concentration ($mg.L^{-1}$), K_L ($L.mg^{-1}$) is the Langmuir adsorption constant. Figure 4(a) shows the linear Langmuir isotherm plot (C_e/q_e versus C_e) for Cu(II) adsorption on the GO surface. The q_m and K_L values obtained from the Langmuir isotherm plot were 324 $mg.g^{-1}$ and 9.61 $L.mg^{-1}$, respectively; R^2 was 0.996.

The Freundlich isotherm is an empirical model used for multilayer adsorption and assumes that adsorption occurs on heterogeneous surfaces. The Freundlich isotherm is given as follows (Sadeek, Negm, Hefni, & Wahab, 2015):

$$\ln q_e = \ln k_F + \frac{1}{n} \ln c_e \qquad (5)$$

where K_F is the Freundlich constant ($L.g^{-1}$) and n is a constant related to adsorption intensity. The linear plot of $\ln q_e$ versus $\ln c_e$ for the adsorption isotherm of Cu(II) on the GO surface is shown in Figure 4b. The K_F and n values calculated from the intercept and slope were 230 L^{-1} mg and 4.42, respectively; R^2 was 0.993. The value of n was greater than 1, indicating a favorable adsorption process.

The Temkin isotherm assumes that the heat of adsorption of molecules in the layer decreases linearly as surface coverage increases because of adsorbent-adsorbate interactions. The Temkin model equation is given as (Oladoja, Aboluwoye, & Oladimeji, 2008):

$$q_e = B \ln k_T + B \ln c_e \qquad (6)$$

where B is a constant related to the heat of adsorption ($Jmol^{-1}$), and □□ is the Temkin isotherm constant ($L.g^{-1}$). The linear Temkin isotherm plot (q_e vs. ln C_e) is displayed in Figure 4c. The constants K_T and B were obtained from the intercept and slope, respectively: □□ = 391.34 and B = 42.409; R^2 = 0.969.

The Langmuir, Freundlich, and Temkin isotherm parameters are listed in Table 2. The Langmuir model had the highest correlation coefficient (R^2), indicating that it provided the best fit to the adsorption data and that Cu(II) adsorption on GO occurred as monolayer coverage. The maximum Cu(II) adsorption capacity, q_m, calculated from the Langmuir model was 324 $mg.g^{-1}$. This value is higher than values reported in the literature (Cui et al., 2015; Mi et al., 2012; Tan et al., 2017; Tan et al., 2015; Wang et al., 2018; White et al., 2018; W. Wu et al., 2013; Yi et al., 2017). Numerous studies have used GO as an adsorbent for Cu(II). Differences in the reported maximum adsorption capacities may be attributed to variations in GO preparation conditions, such as the degree of graphite oxidation (Tan et al., 2017), as well as differences in experimental conditions, including the initial Cu(II) concentration, GO dose, solution pH, and temperature (White et al., 2018; Yi et al., 2017).

Table (2). Adsorption isotherm parameters

Langmuir isotherm		Freundlich isotherm		Temkin isotherm	
K_L ($L.mg^{-1}$)	9.611	K_F	230	K_T ($L.g^{-1}$)	391.34
q_{max}($mg.g^{-1}$)	324	n	4.42	B ($J.mol^{-1}$)	42.41
R^2	0.996	R^2	0.993	R^2	0.969

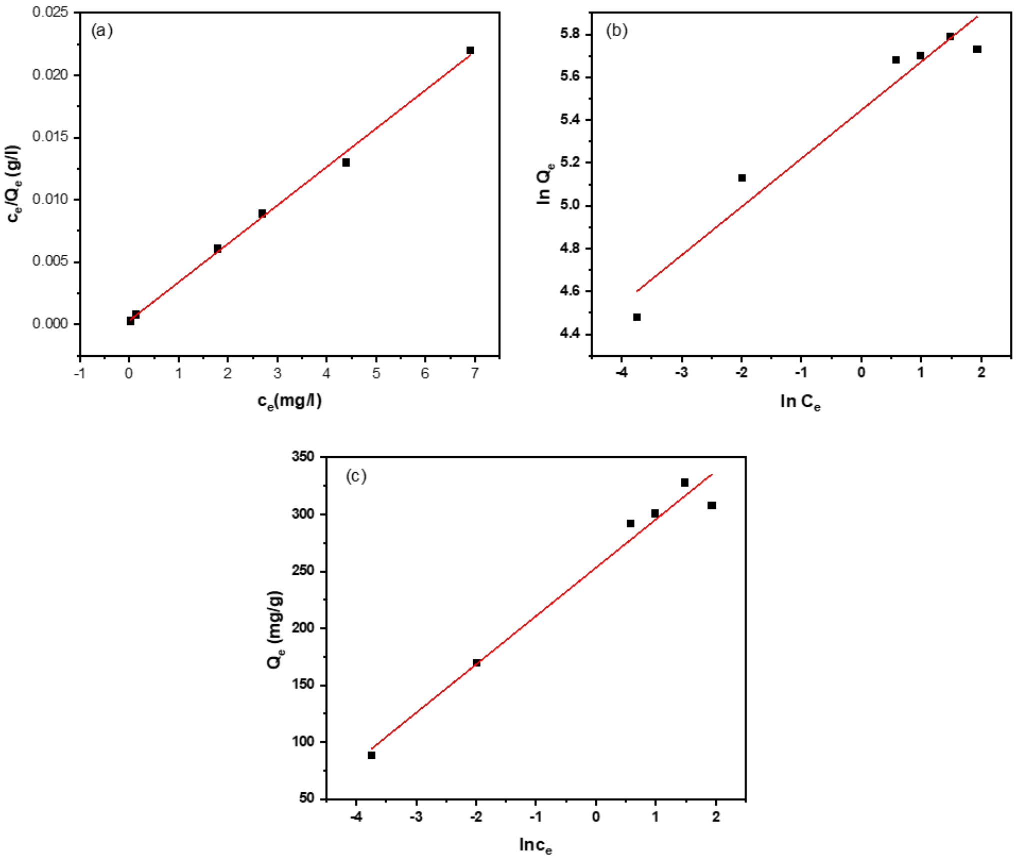

Figure (4): Adsorption isotherms of Cu(II) on the GO surface: (a) Langmuir isotherm, (b) Freundlich isotherm, (c) Temkin isotherm.

Thermodynamic Analysis

The thermodynamic parameters, including entropy change (ΔS°), Gibbs free energy change (ΔG°), and enthalpy change (ΔH°), for Cu(II) adsorption on GO were evaluated using the following equations:

$$lnK_d = \frac{\Delta S^{\circ}}{R} - \frac{\Delta H^{\circ}}{RT} \quad (7)$$

$$\Delta G^{\circ} = \Delta H^{\circ} - T\Delta S^{\circ} \quad (8)$$

where K_d (L.g-1) is the distribution constant, R is the universal gas constant (8.314 J mol−1 K−1), and T is the absolute temperature (K). The $K_d = \frac{q_e}{c_e}$parameters ΔH° and ΔS° were calculated from

the slope and intercept, respectively, of the plot of ln K_d versus 1/T. Table 3 summarizes the thermodynamic parameters. The positive ΔH° value indicates that Cu(II) adsorption on the GO surface is endothermic; ΔH° was lower than 40 kJ.mol-1, which indicates physisorption (Kara, Yuzer, Sabah, & Celik, 2003; C.-H. Wu, Kuo, & Guan, 2016). The ΔS° value was also positive, indicating increased randomness at the solid/liquid interface. A negative value of ΔG° indicates the feasibility and spontaneity of the adsorption process (Guerrero-Fajardo, Giraldo, & Moreno-Piraján, 2020).

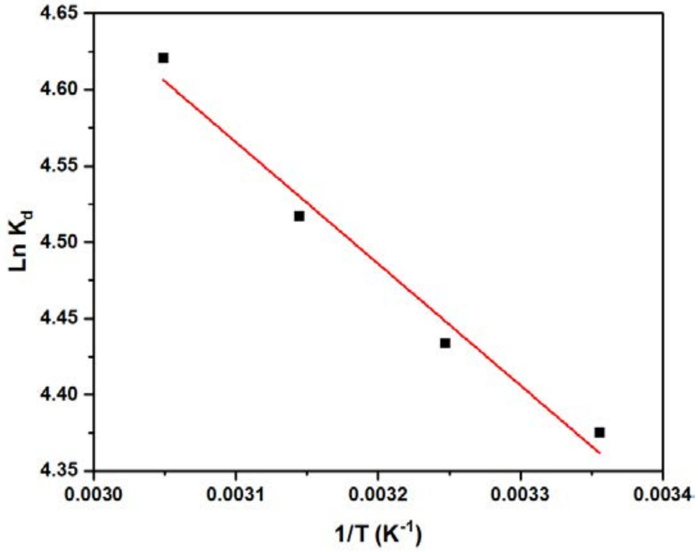

Figure (5). Plot of ln Kd vs. 1/T for adsorption of Cu(II) on the GO surface.

Table (3). Thermodynamic parameters

T (K)	ΔH° $kJ.mol^{-1}$	ΔS° $kJ.mol^{-1} K^{-1}$	ΔG° ($kJ\ mol^{-1}$)
298	6.634	0.0585	-10.799
308			-11.418
318			-11.969
328			-12.554

CONCLUSION

Successful preparation of GO via a modified Hummers method was confirmed by FT-IR and XRD analyses. GO was an efficient adsorbent for the removal of Cu(II) ions from aqueous solutions. The kinetic parameters were determined using pseudo-first-order and pseudo-second-order kinetic models. The results showed that the adsorption process followed the pseudo-second-order kinetic model. Adsorption equilibrium was evaluated using the Langmuir, Freundlich, and Temkin isotherm models. The adsorption equilibrium data were best described by the Langmuir isotherm. The maximum monolayer adsorption capacity obtained from the Langmuir isotherm was 324 $mg.g^{-1}$. The thermodynamic parameters ΔG◦, ΔH◦, and ΔS◦ indicated that the adsorption process was spontaneous and endothermic. These findings highlight GO as a promising adsorbent for heavy metal ion removal from water, with potential applications in environmental remediation.

ACKNOWLEDGEMENT

We wish to thank the Chemistry Department of Sebha University for supporting us.

Duality of interest: The authors declare that they have no duality of interest associated with this manuscript.

Author contributions: Raja Izriq was responsible for methodology, writing, reviewing, and editing the manuscript; Rokaya Azaga contributed to writing; Mohammed S. Ibrahim contributed to reviewing and editing; Hamd Moamen conducted the experiments.

Funding: No specific funding was received for this work.

References

Abu-Dief, A. M., Abdel-Rahman, L. H., Abd–ElSayed, M., & Zikry, M. M. (2021). Green synthesis of silver nanoparticles using Delonix regia extract, characterization and its application as adsorbent for removal of Cu (II) ions from aqueous solution. *Asian Journal of Applied Chemistry Research*, *9*(1), 1-15. DOI: 10.9734/ajacr/2021/v9i130202

Ahmed, S., Choudhury, T. R., Alam, M. Z., & Nurnabi, M. (2023). Adsorption of Cu (II) and Cd (II) with graphene based adsorbent: adsorption kinetics, isotherm and thermodynamic studies. *Desalination and Water Treatment*, *285*, 167-179 https://doi.org/10.5004/dwt.2023.29290.

Ali, A. H., Kareem, A. B., Al-Rawi, U. A., Khalid, U., Zhang, S., Zafar, F., . . .& Sher, F. (2023). Kinetic and equilibrium study of graphene and copper oxides modified nanocomposites for metal ions adsorption from binary metal aqueous solution. *Frontiers in Chemistry*, *11*, 1279948. https://doi.org/10.3389/fchem.2023.1279948

Ayach, J., El Malti, W., Duma, L., Lalevée, J., Al Ajami, M., Hamad, H., & Hijazi, A. (2024). Comparing conventional and advanced approaches for heavy metal removal in wastewater treatment: an in-depth review emphasizing filter-based strategies. *Polymers*, *16*(14), 1959. https://doi.org/10.3390/polym16141959

Benalia, M. C., Youcef, L., Bouaziz, M. G., Achour, S., & Menasra, H. (2022). Removal of heavy metals from industrial wastewater by chemical precipitation: mechanisms and sludge characterization. *Arabian Journal for Science and Engineering*, *47*(5), 5587-5599. https://doi.org/10.3390/polym16141959

Chen, J., Li, Y., Huang, L., Li, C., & Shi, G. (2015). High-yield preparation of graphene oxide from small graphite flakes via an improved Hummers method with a simple purification process. *Carbon*, *81*, 826-834. 10.1016/j.carbon.2014.10.033

Cui, L., Wang, Y., Gao, L., Hu, L., Yan, L., Wei, Q., & Du, B. (2015). EDTA functionalized magnetic graphene oxide for removal of Pb (II), Hg (II) and Cu (II) in water treatment: adsorption mechanism and separation property. *Chemical Engineering Journal*, *281*, 1-10. 10.1016/j.cej.2015.06.043

Dawam, M., Gobara, M., Oraby, H., Y. Zorainy, M., & Nabil, I. M. (2025). Advances in membrane technologies for heavy metal removal from polluted water: A comprehensive review. *Water, Air, & Soil Pollution*, *236*(7), 461. https://doi.org/10.1007/s11270-025-08035-6

Deng, H., Wei, W., Yao, L., Zheng, Z., Li, B., Abdelkader, A., & Deng, L. (2022). Potential-mediated recycling of copper from brackish water by an electrochemical copper pump. *Advanced Science*, *9*(30), 2203189. https://doi.org/10.1002/advs.202203189Digital Object Identifier (DOI)

Deshwal, N., Singh, M. B., Bahadur, I., Kaushik, N., Kaushik, N. K., Singh, P., & Kumari, K. (2023). A review on recent advancements on removal of harmful metal/metal ions using graphene oxide: Experimental and theoretical approaches. *Science of the Total Environment*, *858*, 159672. https://doi.org/10.1016/j.scitotenv.2022.159672

Dutta, S., Gupta, B., Srivastava, S. K., & Gupta, A. K. (2021). Recent advances on the removal of dyes from wastewater using various adsorbents: A critical review. *Materials Advances, 2*(14), 4497-4531. https://doi.org/10.1039/d1ma00354b

Elewa, A., Amer, A., Attallah, M., Gad, H., Al-Ahmed, Z., & Ahmed, I. (2023). Chemically activated carbon based on biomass for adsorption of Fe (III) and Mn (II) ions from aqueous solution. Materials, 16 (3), 1251. https://doi.org/10.3390/ma16031251

Emiru, T. F., & Ayele, D. W. (2017). Controlled synthesis, characterization and reduction of graphene oxide: A convenient method for large scale production. *Egyptian Journal of Basic and Applied Sciences, 4*(1), 74-79. https://doi.org/10.1016/j.ejbas.2016.11.002

Gomes, B. F. M. L., de Araújo, C. M. B., do Nascimento, B. F., Freire, E. M. P. d. L., Da Motta Sobrinho, M. A., & Carvalho, M. N. (2022). Synthesis and application of graphene oxide as a nanoadsorbent to remove Cd (II) and Pb (II) from water: adsorption equilibrium, kinetics, and regeneration. *Environmental Science and Pollution Research, 29*(12), 17358-17372. https://doi.org/10.1007/s11356-021-16943-3

Guerrero-Contreras, J., & Caballero-Briones, F. (2015). Graphene oxide powders with different oxidation degree, prepared by synthesis variations of the Hummers method. *Materials Chemistry and Physics, 153*, 209-220. https://doi.org/10.1016/j.matchemphys.2015.01.005

Guerrero-Fajardo, C. A., Giraldo, L., & Moreno-Piraján, J. C. (2020). Preparation and characterization of graphene oxide for Pb (II) and Zn (II) ions adsorption from aqueous solution: Experimental, thermodynamic and kinetic study. *Nanomaterials, 10*(6), 1022. https://doi.org/10.3390/nano10061022

Gupta, V. K., Carrott, P. J. M., Ribeiro Carrott, M. M. L., & Suhas. (2009). Low-cost adsorbents: growing approach to wastewater treatment—a review. *Critical reviews in environmental science and technology, 39*(10), 783-842. https://doi.org/10.1080/10643380801977610

Hu, X. J., Liu, Y. G., Wang, H., Chen, A. W., Zeng, G. M., Liu, S. M., ... & Liu, S. H. (2013). Removal of Cu (II) ions from aqueous solution using sulfonated magnetic graphene oxide composite. *Separation and Purification Technology, 108*, 189-195. https://doi.org/10.1016/j.seppur.2013.02.011

Imamoglu, M., & Tekir, O. (2008). Removal of copper (II) and lead (II) ions from aqueous solutions by adsorption on activated carbon from a new precursor hazelnut husks. *Desalination, 228*(1-3), 108-113. https://doi.org/10.1016/j.desal.2007.08.011

Kara, M., Yuzer, H., Sabah, E., & Celik, M. (2003). Adsorption of cobalt from aqueous solutions onto sepiolite. *Water research, 37*(1), 224-232. https://doi.org/10.1016/S0043-1354(02)00265-8

Katiyar, R., Patel, A. K., Nguyen, T.-B., Singhania, R. R., Chen, C.-W., & Dong, C.-D. (2021). Adsorption of copper (II) in aqueous solution using biochars derived from Ascophyllum nodosum seaweed. *Bioresource technology, 328*, 124829. 10.1016/j.biortech.2021.124829

Kaushal, A., Dhawan, S. K., & Singh, V. (2019). Determination of crystallite size, number of graphene layers and defect density of graphene oxide (GO) and reduced graphene oxide (RGO). *In AIP Conference Proceedings*, 2115(1), 030106. https://doi.org/10.1063/1.5112945

Khan, M., Muhammad, M., AlOthman, Z. A., Cheong, W. J., & Ali, F. (2022). Synthesis of monolith silica anchored graphene oxide composite with enhanced adsorption capacities for carbofuran and imidacloprid. *Scientific Reports*, *12*(1), 21027. https://doi.org/10.1038/s41598-022-25528-0

Kumar, A. S. K., & Jiang, S.-J. (2016). Chitosan-functionalized graphene oxide: A novel adsorbent an efficient adsorption of arsenic from aqueous solution. *Journal of environmental chemical engineering*, *4*(2), 1698-1713. https://doi.org/10.1016/j.jece.2016.02.035

Liu, Y., Zhong, Q., & Zhang, T. (2015). Preparation of cationic surfactant intercalated graphene oxide and quantitative determination of the interlamellar spacing. *Fullerenes, Nanotubes and Carbon Nanostructures*, *23*(3), 196-202. https://doi.org/10.1080/1536383X.2013.787598

Daniela C. Marcano, Dmitry V. Kosynkin, Jacob M. Berlin, Alexander Sinitskii, Zhengzong Sun, Alexander Slesarev, Lawrence B. Alemany, Wei Lu, James M. Tour; Improved Synthesis of Graphene Oxide. *ACS Nano* 24 August 2010; 4 (8): 4806–4814. https://doi.org/10.1021/nn1006368

Mi, X., Huang, G., Xie, W., Wang, W., Liu, Y., & Gao, J. (2012). Preparation of graphene oxide aerogel and its adsorption for Cu^{2+} ions. *Carbon*, *50*(13), 4856-4864. 10.1016/j.carbon.2012.06.013

Musah, M., Azeh, Y., Mathew, J. T., Umar, M. T., Abdulhamid, Z., & Muhammad, A. I. (2022). Adsorption kinetics and isotherm models: a review. *CaJoST*, *4*(1), 20-26. https://dx.doi.org/10.4314/cajost.v4i1.3

Nassef, H. M., Al-Hazmi, G. A., Alayyafi, A. A., El-Desouky, M. G., & El-Bindary, A. A. (2024). Synthesis and characterization of new composite sponge combining of metal-organic framework and chitosan for the elimination of Pb (II), Cu (II) and Cd (II) ions from aqueous solutions: Batch adsorption and optimization using Box-Behnken design. *Journal of Molecular Liquids*, *394*, 123741. 10.1016/j.molliq.2023.123741

Oladoja, N., Aboluwoye, C., & Oladimeji, Y. (2008). Kinetics and Isotherm Studies on Methylene Blue Adsorption onto Ground Palm Kernel Coat. *Turkish Journal of Engineering & Environmental Sciences*, *32*(5).

Raji, Z., Karim, A., Karam, A., & Khalloufi, S. (2023). Adsorption of heavy metals: mechanisms, kinetics, and applications of various adsorbents in wastewater remediation—a review. *Waste*, 1(3), 775-805). https://doi.org/10.3390/waste1030046

Rathore, E., & Biswas, K. (2018). Selective and ppb level removal of Hg (ii) from water: synergistic role of graphene oxide and SnS 2. *Journal of Materials Chemistry A*, *6*(27), 13142-13152. https://doi.org/10.1039/c8ta02680g

Sadeek, S. A., Negm, N. A., Hefni, H. H., & Wahab, M. M. A. (2015). Metal adsorption by agricultural biosorbents: adsorption isotherm, kinetic and biosorbents chemical structures. *International journal of biological macromolecules*, *81*, 400-409. https://doi.org/10.1016/j.ijbiomac.2015.08.031

Shalaby, A., Nihtianova, D., Markov, P., Staneva, A., Iordanova, R., & Dimitriev, Y. (2015). Structural analysis of reduced graphene oxide by transmission electron microscopy. *Bulgarian Chemical Communications*, *47*(1), 291-295.

Shek, T.-H., Ma, A., Lee, V. K., & McKay, G. (2009). Kinetics of zinc ions removal from effluents using ion exchange resin. *Chemical Engineering Journal, 146*(1), 63-70. doi:10.1016/j.cej.2008.05.019, 1385-8947

Tan, P., Bi, Q., Hu, Y., Fang, Z., Chen, Y., & Cheng, J. (2017). Effect of the degree of oxidation and defects of graphene oxide on adsorption of Cu^{2+} from aqueous solution. *Applied Surface Science, 423*, 1141-1151. https://doi.org/10.1016/j.apsusc.2017.06.304

Tan, P., Sun, J., Hu, Y., Fang, Z., Bi, Q., Chen, Y., & Cheng, J. (2015). Adsorption of Cu^{2+}, Cd^{2+} and Ni^{2+} from aqueous single metal solutions on graphene oxide membranes. *Journal of hazardous materials*, *297*, 251-260. https://doi.org/10.1016/j.jhazmat.2015.04.068

Türkmen, D., Bakhshpour, M., Akgönüllü, S., Aşır, S., & Denizli, A. (2022). Heavy metal ions removal from wastewater using cryogels: A review. *Frontiers in Sustainability*, 3, 765592. https://doi.org/10.3389/frsus.2022.765592

Vieira, M. A., Gonçalves, G. R., Cipriano, D. F., Schettino Jr, M. A., Silva Filho, E. A., Cunha, A. G., . . . & Freitas, J. C. (2016). Synthesis of graphite oxide from milled graphite studied by solid-state 13C nuclear magnetic resonance. *Carbon, 98*, 496-503. https://doi.org/10.1016/j.carbon.2015.11.037.

Viprya, P., Kumar, D., & Kowshik, S. (2023). Study of different properties of graphene oxide (GO) and reduced graphene oxide (rGO). *Engineering Proceedings, 59*(1), 84. https://doi.org/10.3390/engproc2023059084

Wang, H., Hu, X., Guo, Y., Qiu, C., Long, S., Hao, D., Cai, X., Xu, W., Wang, Y. and Liu, Y. (2018), Removal of copper ions by few-layered graphene oxide nanosheets from aqueous solutions: external influences and adsorption mechanisms. *J. Chem. Technol. Biotechnol*, 93: 2447-2455. https://doi.org/10.1002/jctb.5601

White, R. L., White, C. M., Turgut, H., Massoud, A., & Tian, Z. R. (2018). Comparative studies on copper adsorption by graphene oxide and functionalized graphene oxide nanoparticles. *Journal of the Taiwan Institute of Chemical Engineers, 85*, 18-28. https://doi.org/10.1016/j.jtice.2018.01.036

Wu, C.-H., Kuo, C.-Y., & Guan, S.-S. (2016). Adsorption of heavy metals from aqueous solutions by waste coffee residues: kinetics, equilibrium, and thermodynamics. *Desalination and Water Treatment*, *57*(11), 5056-5064. https://doi.org/10.1080/19443994.2014.1002009

Wu, W., Yang, Y., Zhou, H., Ye, T., Huang, Z., Liu, R., & Kuang, Y. (2013). Highly efficient removal of Cu (II) from aqueous solution by using graphene oxide. *Water, Air, & Soil Pollution*, *224*(1), 1372. https://doi.org/10.1007/s11270-012-1372-5

Xue, B., Zhu, J., Liu, N., & Li, Y. (2015). Facile functionalization of graphene oxide with ethylenediamine as a solid base catalyst for Knoevenagel condensation reaction. *Catalysis Communications*, *64*, 105-109. https://doi.org/10.1016/j.catcom.2015.02.003

Yi, I.-G., Kang, J.-K., Kim, J.-H., Lee, S.-C., Sim, E.-H., Park, J.-A., & Kim, S.-B. (2017). Adsorption characteristics of graphene oxide in the removal of Cu (II) from aqueous solutions. *Desalination and Water Treatment*, *72*, 308-317. https://doi.org/10.5004/dwt.2017.20651